Available online at www.sciencedirect.com
SCIENCE DIRECT®
Journal of Power Sources 119–121 (2003) 844–849
JOURNAL OF POWER SOURCES
www.elsevier.com/locate/jpowsour

Heats of mixing and of entropy in porous insertion electrodes

Karen E. Thomas, John Newman*

Lawrence Berkeley National Laboratory, Energy and Environmental Technologies Division and Department of Chemical Engineering, University of California, Berkeley, CA 94720, USA

Abstract

Heat is produced after interruption of the current because of relaxation of concentration gradients in electrochemical systems. This heat of relaxation is termed heat of mixing. Two methods, one computational and one analytic approximation, for computing the heat of mixing are presented. In general, the magnitude of the heat of mixing will be small in materials with transport properties sufficiently high to provide acceptable battery performance, with the possible exception of heat of mixing within the insertion particles if the particle radius is large.

In insertion materials, such as lithium insertion electrodes, the entropy of reaction may vary substantially with state of charge. The entropy of reaction accounts for a reversible heat effect which may be of the same order of magnitude as the resistive heating. Measurements for the entropy of reaction as a function of state of charge in $LiCoO_2$, $LiNi_{0.8}Co_{0.2}O_2$, and LiC_6 are presented.

Keywords: Thermal model; Entropy; Heat of mixing

1. Introduction

In this paper, we address two separate aspects of heat generation in insertion electrodes. The first aspect is heat of mixing, which relates to the heat generated by the system during relaxation after the current is turned off. We discuss how to calculate this heat of relaxation. The second aspect is the entropy of reaction, which relates to the reversible heat produced during passage of current. We present measurements of the entropy of reaction for several materials currently of interest for lithium-ion batteries.

Heat of mixing in porous insertion electrodes has not been treated in detail previously. Bernardi et al. [1] present a completely general energy balance for an electrochemical system, assuming only that the temperature is uniform and neglecting effects of pressure. The authors had in mind a main reaction that was a phase change reaction, and therefore do not explicitly discuss heat of mixing effects within the electrode, although such effects are implicitly present in their heat of mixing term. Lithium-ion batteries use insertion electrodes, which are solid solutions. Since concentration gradients develop within the particles of insertion material during passage of current, and the partial molar enthalpy does vary with lithium concentration, there will be heat of mixing in these materials. Rao and Newman [2] developed an energy balance which accounts more explicitly for the fact that the potential varies with lithium concentration in insertion compounds. However, as will be shown below, they do not treat heat of mixing consistently. Their final equation (Eq. (17)) includes heat of mixing across a porous electrode, but not within the spherical particles of insertion material or in the electrolyte. Since these different components of heat of mixing may all be of equal magnitude but of possibly different sign, including only one component of the heat of mixing in the energy balance is not consistent.

The entropy of reaction of a nonstoichiometric insertion reaction is equal to $(\partial S/\partial y)_{T,P}$, where S is the total entropy of the insertion electrode and y the extent of reaction, and also is equal to $(nF(\partial U)/(\partial T))_{y,P}$, where U is the open-circuit potential of the insertion electrode with respect to a reference electrode, n the number of electrons transferred, and F Faraday's constant. For convenience, we refer to the entropy of reaction as $\partial U/\partial T$. For a lithium-ion cell, the thermodynamic potential of both the positive and the negative electrode varies as a function of lithium concentration. Therefore, to calculate the rate of heat generation from a lithium-ion cell, one must know U and $\partial U/\partial T$ as a function of state of charge for each insertion electrode, measured with respect to the same reference electrode, such as lithium metal.

A positive $\partial U/\partial T$ indicates that passage of an incremental amount of charge increases the disorder of the system. In a nearly empty lattice, there are few possible

* Corresponding author. Tel.: +1-510-642-4063; fax: +1-510-642-4778.
E-mail address: newman@newman.cchem.berkeley.edu (J. Newman).

0378-7753/03/$ – see front matter © 2003 Published by Elsevier Science B.V.
doi:10.1016/S0378-7753(03)00283-0

configurations for the lithium atoms. Then the entropy change of adding a few lithium atoms would be positive; since the lithium could reside on any of the many available sites, the partially filled lattice has higher total entropy than the empty lattice. When all of the sites of similar energy are almost full, insertion of additional lithium creates a more ordered state (a full lattice), and $\partial U/\partial T$ would be negative. We have reported measurements previously for lithium–manganese-oxide spinels that follow this pattern of positive $\partial U/\partial T$ decreasing to negative $\partial U/\partial T$ as sites are filled [3]. Some insertion compounds undergo a first-order phase change over some range of lithium concentration. During a first-order phase transition, the entropy of reaction will be constant with state of charge by the Gibbs phase rule.

2. Experimental methods

Coin cells were assembled in a helium-filled dry box using 1 M $LiPF_6$ in 1:1 ethylene carbonate:dimethyl carbonate (Merck Selectipur) electrolyte, Celgard 3401, 3501, or 2400 separator, and a lithium metal counterelectrode. $LiCoO_2$ electrodes were obtained from Quallion (Sylmar, CA). $LiNi_{0.8}Co_{0.2}O_2$ electrodes were obtained from PolyStor (Livermore, CA), containing 84% $LiNi_{0.8}Co_{0.2}O_2$, 4% SFG 6 graphite, 4% Chevron C/55 carbon black, and 8% PVdF on aluminum-foil current collectors. Graphite mesocarbon microbead (MCMB), synthesized at 2800 K, electrodes were obtained in coin cells from Telcordia and from PolyStor, both using copper current collectors. The Telcordia electrodes contained 88.3 wt.% 25 μm diameter MCMB particles, 3.1% Super P carbon black, and 8.6% PVdF. The PolyStor electrodes contained 91.5 wt.% 6 μm diameter MCMB particles and 8.5% PVdF.

The cell was wrapped in one layer of polyethylene and placed in a water bath whose temperature was 298 K unless otherwise noted. To reduce the thermal mass of the cell, leads were epoxied to the case using electronically conductive epoxy.

The open-circuit potential was estimated from data for two charge-discharge cycles at the C/48 or C/25 rate. The lithium stoichiometry, y, was calculated from the amount of charge passed and the measured mass of active material, corrected for side reactions (which consumed about 0.1% of the total charge passed) by the method of Darling and Newman [4].

The entropy was measured by varying the temperature of the cell at open circuit and recording the cell potential as a function of temperature. The temperature of the cell was varied by a VWR PolyScience model 1147 water bath controlled by a Macintosh computer using the same LabVIEW program that controlled the EG&G 273 potentiostat and HP 3458A multimeter. The temperature was ramped at approximately 0.3 °C/min between 21 and 29 °C. In electrodes at very oxidizing or very reducing potentials, the potential drops substantially during relaxation due to the increased rate of self discharge and the high slope of $U(y)$. The potential changes with time because the state of charge is decreasing as self discharge occurs. This potential change is superimposed upon the potential change that occurs as the temperature of the cell is varied, introducing error into the calculation of $\partial U/\partial T$. To correct the continual decrease in potential over the course of the temperature cycling, the variation of potential with time at constant temperature during relaxation was subtracted from the variation of potential with time during temperature variation [3]. The differential potential then yielded a straight line when plotted against temperature. The subtraction of the potential profile during relaxation at constant temperature from the potential profile during relaxation at changing temperature allows accurate measurements of $\partial U/\partial T$ even at high states of charge.

3. Calculation of the heat of relaxation

The energy balance commonly used in the literature to describe electrochemical systems is:

$$\dot{Q} = I\left(V - U + T\frac{\partial U}{\partial T}\right) + C_p\frac{\mathrm{d}T}{\mathrm{d}t} \tag{1}$$

where $\dot{Q}$ is the rate of heat transferred from the surroundings to the system, I the current (positive on discharge), V the cell potential, U the open-circuit potential evaluated at the average state of charge in the electrodes, T the temperature, and C_p the heat capacity [1,5,6]. By this equation, generation of heat will cease the instant the current is turned off. However, we know from experience with calorimetry that this is not the case; after the current is turned off, some amount of heat continues to be released (or, in some cases, absorbed). Why?

To answer this question, let us think of why heat is generated at all in an electrochemical system. If current were passed infinitesimally slowly, then the cell would remain at equilibrium, i.e. V would be the same as U, and the only heat generated would be the reversible heat of reaction, $IT(\partial U/\partial T) = T(\mathrm{d}S/\mathrm{d}t)$. This heat can be either exothermic or endothermic, depending on the entropy of reaction and direction of current.

In reality, the current is nonzero, and the cell voltage is displaced from its equilibrium potential because of the resistance in the cell to the passage of current. The rate of energy loss to resistive dissipation is therefore $I(V - U)$. This heat is always exothermic.

In addition, there is a resistance to mass transport in the system, leading to the formation of concentration gradients as ions are moved through the electrolyte from one electrode to the other and as products are formed by electrochemical reaction at the interface between the electrolyte and particles of insertion material. When the current is turned off, these concentration gradients relax, and the relaxation is accompanied by a sensible heat effect. Thus, heat is exchanged

during formation of concentration gradients as current is passed, and an equal and opposite amount of heat is exchanged upon relaxation of those gradients. This heat is termed as the heat of mixing, and it is this heat which is observed as the heat of relaxation after the current is turned off.

Eq. (1) does conserve energy. However, it does not exactly describe when heat is generated, because it ignores heat involved in formation of concentration gradients. A rederivation of the energy balance [1,7] for an electrochemical system yields the equation:

$$\dot{Q} = \left(IV - \sum_l I_l U_l^{\text{avg}} \right) + \sum_l I_l T \frac{\partial U_l^{\text{avg}}}{\partial T} + C_\text{p} \frac{\text{d}T}{\text{d}t} + \sum_k \triangle H_k^{\text{avg}} r_k + \int \sum_j \sum_i (\bar{H}_{ij} - \bar{H}_{ij}^{\text{avg}}) \frac{\partial c_{ij}}{\partial t} \, \text{d}v \quad (2)$$

where $\bar{H}_{ij}^{\text{avg}}$ is the partial molar enthalpy evaluated at the volume-averaged concentration at any point in time, c is the concentration, and we have allowed for any number of electrochemical reactions l and chemical reactions k and for any number of species i in phases j. The first term on the right side is the irreversible resistive heat, the second is the reversible entropic heat, the third is the heat capacity, the fourth is heat change by any chemical reactions that may be present in the cell, and the last is the heat of mixing. Thus, this equation allows one to calculate how much heat the cell will generate during relaxation of concentration gradients. If the partial molar enthalpies are all constant with composition, then the heat-of-mixing term is zero.

There are four types of concentration gradients in batteries with porous insertion electrodes, across the insertion electrode due to nonuniform current distribution, across the electrolyte due to mass transfer, and radially both within the particles of insertion material and within the electrolyte-filled pores because the electrochemical reaction occurs at the interface between electrode and electrolyte. For the purpose of including the energy balance in a full-cell-sandwich simulation of the cell performance, one may find it convenient to divide the heat of mixing terms into separate terms for each of the components of heat of mixing:

$$\dot{Q} = IV + \int \sum_l a i_{n,l} \langle U_{\text{H},l} \rangle \, \text{d}v + C_\text{p} \frac{\text{d}T}{\text{d}t} + \sum_k \triangle H_k^{\text{avg}} r_k + \int \sum_{i,\text{electrolyte}} (\bar{H}_i - \bar{H}_i^{\text{avg}}) \frac{\partial c_i}{\partial t} \, \text{d}v - \int_{\text{particles}} F \left(U_\text{H} \frac{\partial c_\text{s}}{\partial t} - \langle U_\text{H} \rangle \frac{\partial \langle c_\text{s} \rangle}{\partial t} \right) \text{d}v \quad (3)$$

where $U_\text{H} = U - T(\partial U / \partial T)$, a is the surface area per unit volume, i_n the transfer current between electrode and electrolyte, and c_s is the concentration of inserted lithium. The first two terms now include both resistive and entropic heating and heat of mixing across the insertion electrode. Note that $\langle U_\text{H} \rangle$ is the enthalpy potential evaluated at the local average concentration. For a one-dimensional model, this concentration is that averaged over the cross-sectional plane of the electrode, and is computed from the total amount of reaction that has occurred in that plane. Because of this averaging, the heat of mixing within the particles is not included in the first two terms, and is given separately in the last term. This integral must be performed radially over the volumes of the spherical particles, at each point across an electrode. The second-to-last term gives the heat of mixing within the electrolyte, both across the cell and radially within the pores. Actual evaluation of the heat of mixing radially within pores is difficult to calculate, because the pores have a random geometry. Porous electrode theory averages over the radial concentration within the pores. As shown below, for practical systems the radial concentration gradients within the pores are negligibly small, and explicit calculation of the radial component of term is seldom necessary.

As shown above, complete calculation of the heat of mixing requires a rather complicated integral. The heat of mixing is usually small compared to other heat effects such as entropic and resistive heating. However, it is useful to have an estimate of the magnitude of the heat of mixing in cases where large concentration gradients are expected to be produced, such as under passage of a high current density in an electrolyte with poor transport properties and a strong dependence of partial molar enthalpy on concentration. Next, we present a simple closed-form equation to estimate the magnitude of the heat-of-mixing effect for a two-component system.

Consider the situation in which a concentration gradient exists across a solution of two components, A and B, and the concentration gradient is allowed to relax to a uniform concentration of $c_{A,\infty}$ and $c_{B,\infty}$ and temperature T_∞. The total enthalpy of the solution at any time is the sum of the partial molar enthalpies of the components integrated over the volume of the system:

$$H = \int (c_A \bar{H}_A + c_B \bar{H}_B) \, \text{d}v \quad (4)$$

Expand the partial molar enthalpy in a Taylor series about T_∞ and $c_{A,\infty}$. After some manipulation, one can find that the change in enthalpy from the initial, nonuniform state to the final state is then given by:

$$\Delta H = \frac{1}{2 c_{B,\infty} \bar{V}_{B,\infty}} \left. \frac{\partial \bar{H}_A}{\partial c_A} \right|_\infty \int (c_A - c_{A,\infty})^2 \, \text{d}v + C_{p_\infty} \Delta T \quad (5)$$

The assumptions used to derive this equation were the use of a second-order Taylor expansion for the partial molar enthalpy, neglect of the effect of pressure, neglect of the change in density with temperature, and neglect of the effect of the dependence on concentration of the partial molar volumes on the second derivative of the partial molar enthalpy [7].

Eq. (5) allows us to calculate the heat of mixing involved in the relaxation or formation of any known concentration

profile, requiring only data for $\partial\bar{H}_A/\partial c_A$. The sign of the heat of mixing depends solely on the sign of $\partial\bar{H}_A/\partial c_A$. If $\partial\bar{H}_A/\partial c_A$ is positive, then the relaxation of concentration gradients is an exothermic process. Analytic approximations can be obtained for the different kinds of concentration profiles in batteries with porous insertion electrodes to evaluate $\int(c_A - c_{A,\infty})^2\,\mathrm{d}v$. For example, substitution of the pseudo-steady-state concentration profile formed in spherical insertion particles subject to a uniform reaction rate at their surface into Eq. (5) yields the following expression for the amount of heat involved in relaxation of these concentration gradients

$$\Delta H = \frac{1}{1050 c_{\mathrm{matrix},\infty}\bar{V}_{\mathrm{matrix},\infty}}\left.\frac{\partial\bar{H}_\mathrm{s}}{\partial c_\mathrm{s}}\right|_\infty\left(\frac{i}{FD_\mathrm{s}}\right)^2\frac{R^4}{\epsilon_\mathrm{insertion}L} \quad (6)$$

where ΔH is the heat released per unit separator area, D_s diffusion coefficient of lithium in the solid, L the electrode thickness, $\epsilon_\mathrm{insertion}$ the volume fraction of insertion material in the electrode, i the current density, and R the particle radius.

Table 1 shows calculated components of the heat of mixing. Results are presented in terms of ΔH, the heat per unit separator area that would be measured in an isothermal calorimeter. $c_{B,\infty}\bar{V}_{B,\infty}$ was assumed to be equal to 1. For comparison with the heat of mixing, the total heat generated by irreversible resistive heating and reversible entropic heating, calculated from computer simulation, is also given [7].

The cell labeled "liquid" contains a porous insertion electrode of $LiAl_{0.2}Mn_{1.8}O_{4-\delta}F_{0.2}$, $LiPF_6$ in EC: DMC 1:1, and a lithium negative electrode. The electrode dimensions were 174 μm-thick positive electrode, 25.4 μm-thick separator, and 20 μm particle size. Calculations are reported for discharge for 3 h at the C/3 rate (12.29 A/m^2).

The cell labeled "polymer" contains LiV_6O_{13}, lithium bis(trifluoromethylsulfonyl) (LiTFSI) in oxymethylene-linked poly(ethylene oxide) (PEMO), and a lithium negative electrode. The behavior of this cell with several different polymer electrolytes was described by Thomas et al. [8]. Table 1 shows calculations for the polymer which was termed "ideal" polymer electrolyte in that paper, i.e. the transport properties of the polymer electrolyte at 85 °C, under a current density of 10 A/m^2 for 3 h. The enthalpy potential of this material has not been measured. We assume a value of $\partial\bar{H}/\partial c = 10$ Jm^3/mol^2 for lithium–vanadium-oxide in order to calculate the value of the heat of mixing within the particles of the insertion electrode given in Table 1. Heat of mixing across the electrode was calculated using the energy balance of Rao and Newman, but with entropy set to zero since no data are available.

Table 1
Estimated magnitude of the components of heat of mixing during a 3 h discharge

Heat of mixing	$\triangle H$ (J/m^2)	
	Liquid	Polymer
Within particles	22–110	3
Across electrode	0.1–19	52
Across electrolyte	2.0	−52
Within pores	1×10^{-6}	−0.0003
Irreversible + entropic	7520	20160

For comparison, the total resistive and entropic heat produced during the discharge also in shown.

Eq. (5) states that the magnitude of the heat of mixing can be calculated given knowledge of the derivative of partial molar enthalpy with concentration. For the electrolyte, $\partial\bar{H}_\mathrm{salt}/\partial c_\mathrm{salt} = -\nu RT^2\partial^2\ln f_\pm/\partial T\partial c_\mathrm{salt}$, and for the insertion electrode $\partial\bar{H}_\mathrm{s}/\partial c_\mathrm{s} = -F(\partial U_\mathrm{H}/\partial c_\mathrm{s})$ was calculated from numerical differentiation of the data for $U_\mathrm{H}(y)$ of $Li_yAl_{0.2}Mn_{1.8}O_{4-\delta}F_{0.2}$ given in reference [3]. $\partial\bar{H}_\mathrm{s}/\partial c_\mathrm{s}$ ranges from 0 to 24 Jm^3/mol^2.

There are few data in the literature for the activity coefficients of organic electrolytes. Danilova et al. [9] report the activity coefficient of $LiClO_4$ in acetonitrile as a function of concentration at 40 and 60 °C. Based on these data, we calculate that $\partial\bar{H}_\mathrm{salt}/\partial c_\mathrm{salt}$ is 12 Jm^3/mol^2. It is coincidental that all of these materials release heat during the relaxation of concentration gradients. In contrast, data for the polymer electrolyte indicate that heat will be absorbed during relaxation of concentration gradients. Steve Sloop and John Kerr (unpublished) at Lawrence Berkeley National Lab, measured the activity coefficient as a function of concentration at 40, 60, and 85 °C for LiTFSI in PEMO. From these data, we estimate a value of $\partial\bar{H}/\partial c = -50$ Jm^3/mol^2.

From the calculations presented in Table 1, one can draw several general conclusions. Heat of mixing is small relative to resistive and entropic heat in well-designed cells. Heat of mixing within particles can be significant, particularly for large particles, high current density, low solid diffusivity, and a large variation of U_H with concentration. Because concentration gradients in the radial direction within pores are so small, that component of heat of mixing is negligible. A highly nonuniform current distribution, leading to heat of mixing across the electrode, will often be accompanied by large concentration gradients across the electrolyte, causing heat of mixing across the electrolyte.

4. Entropy measurements

$LiCoO_2$ has a layered rock-salt structure consisting of alternating layers of oxygen, cobalt, oxygen, and lithium atoms of space group $R\bar{3}m$. The phase structure as a function of lithium concentration was determined by Reimers and Dahn [10] by using X-ray diffraction and differential capacity plots, complemented by the electronic and NMR studies of Menétrier et al. [11]. From $0.93 < y < 1.0$, the compound is a single-phase solid solution. From $0.75 < y < 0.93$, a phase transition occurs between two hexagonal phases with very similar lattice parameters. The phase transition is observable electrochemically by the voltage plateau at

3.93 V over this composition range. The difference between the two phases is that $Li_{0.93}CoO_2$ is a semiconductor, whereas $Li_{0.75}CoO_2$ is metallic. Van der Ven et al. [12] suggest that the additional configurational entropy of delocalizing the electrons may be the driving force for the semiconductor–metal phase transition. Below $y = 0.75$, the compound is single phase, with the exception that at $y = 0.5$, an order–disorder transition occurs which creates a monoclinic phase with a narrow range of stoichiometry. In the monoclinic phase, it is believed that the lithium atoms within a layer are aligned in rows of lithium atoms alternating with rows of vacancies [10,12]. This order–disorder transition is observable electrochemically as a steep variation of U with y at $y = 0.5$, between two small potential plateaus at 4.07 and 4.19 V.

The stoichiometry of these phase transitions has been verified theoretically [12], but electrochemical determinations of the exact lithium stoichiometry have varied by ± 0.05, perhaps owing to the occurrence of side reactions, error in the mass of active material, or imperfect accessibility of the active material [10,11]. The range of y for the Quallion $LiCoO_2$ electrodes, according to the current passed and the active mass reported by the manufacturer, was 0.52–1.0. Since this range was corrected already for side reactions, it is likely that any error is in the reported mass of active material or that some of this active material was electrically disconnected. The range of y should be 0.45–1.0 to be consistent with the phase diagram of Reimers and Dahn [10], so that the order–disorder transition would occur at $y = 0.5$, as predicted by ab initio calculations [12]. To make our results consistent with the literature, the following discussion assumes that the phase diagram of Reimers and Dahn is correct, and gives our calculated stoichiometries in parentheses.

The open-circuit potential and entropy are shown in Fig. 1. The positions of the three plateaus in the open-circuit potential, at 4.18, 4.06, and 3.91 V, agree with those described above. The order–disorder transition at $y = 0.5$ (0.56 from the measured current and reported active mass) causes a strong variation in the entropy from -0.6 to $+0.3$ mV/K. The entropy decreases continuously from $y = 0.65$ to 0.85 (0.84), and then is constant at -0.6 mV/K during the first-order phase transition from metal to semiconductor from $y = 0.85$ (0.84) to 1.0.

The overall magnitude and range of the entropy in lithium–cobalt-oxide is the largest of all the materials studied in this investigation, indicating that reversible heat generation will be highly significant and vary strongly with state of charge in cells containing $LiCoO_2$ electrodes.

The electronic and crystal structure of $Li_yNi_{0.8}Co_{0.2}O_2$ has been analyzed in detail by Saadoune and Delmas [13]. Like $LiNiO_2$ and $LiCoO_2$, $LiNi_{0.8}Co_{0.2}O_2$ has a layered crystal structure of space group $R\bar{3}m$, with alternating layers in the pattern Li–O–M–O, where the M layer contains both nickel and cobalt. Unlike $LiNiO_2$ or $LiCoO_2$, no phase change occurs upon deintercalation. Saadoune and Delmas

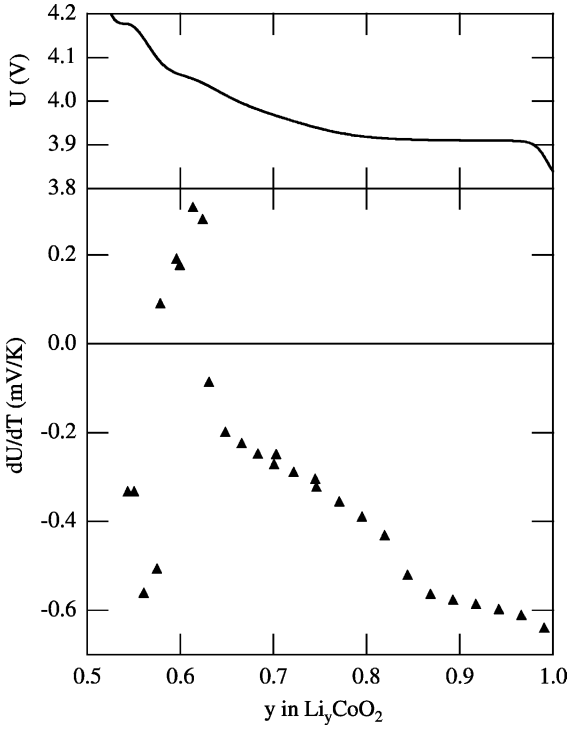

Fig. 1. Open-circuit potential and entropy for Li_yCoO_2.

show that the presence of the cobalt atoms frustrates lithium ordering within the layers, thereby inhibiting a phase change and also inhibiting any long-range ordering of lithium within the lattice. Fig. 2 shows the open-circuit potential and

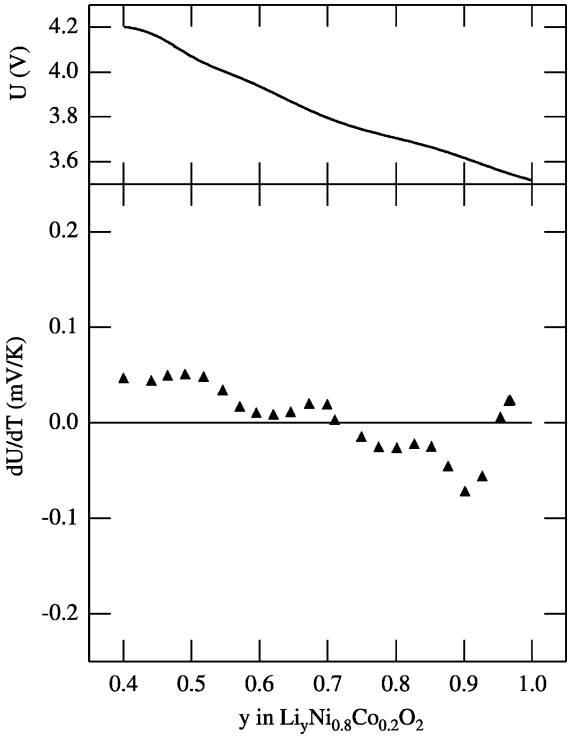

Fig. 2. Open-circuit potential and entropy in $Li_yNi_{0.8}Co_{0.2}O_2$.

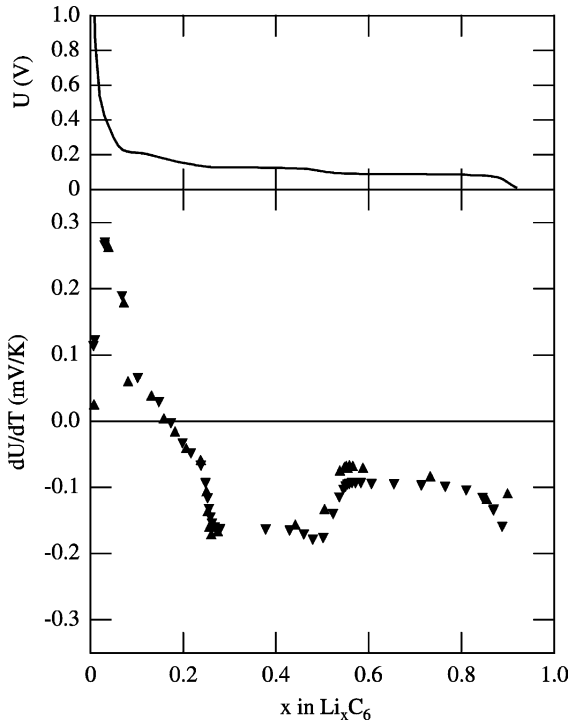

Fig. 3. Open-circuit potential and entropy in MCMB graphite.

entropy measurements for $Li_yNi_{0.8}Co_{0.2}O_2$. In agreement with the results of Saadoune and Delmas, there is no plateau to indicate a phase change, and the pattern roughly follows what would be expected for a solid solution with lithium occupying a lattice in which all lithium sites are equivalent: positive $\partial U/\partial T$ when the lattice is nearly empty, decreasing to negative $\partial U/\partial T$ when the lattice is nearly full. In addition, the magnitude of the entropy of reaction is very small, ranging from −0.08 to 0.06 mV/K, indicating that a change in lithium concentration yields merely a small change in the number of configurations for lithium on the lattice. Because of the extremely small magnitude of the measured entropy, the small rises and dips within the overall downward trend are within the experimental error and should not be considered significant.

Lithium intercalation into graphite occurs by the formation of ordered stages. The stage number indicates the number of graphite layers between lithium layers. The materials examined in this study were synthesized at 2800 K and are therefore fully graphitized.

According to Zheng and Dahn [14,15], at 298 K the phase diagram consists of a single phase of dilute stage 1 (denoted stage 1′) for $0 < x < 0.04$; two-phase transition from stage 1′ to a mixture of stages 4L and 3L for $0.04 < x < 0.12$; an unclear, perhaps single-phase solid solution varying from stage 4L to 3L for $0.12 < x < 0.21$; two-phase transition from stage 3L to 2L for $0.21 < x < 0.25$; two-phase transition between stages 2L and 2 for $0.25 < x < 0.5$; and finally a two-phase transition from stage 2 to 1 for $0.5 < x < 1.0$. The notation "stage nL", such as stages 4L, 3L, and 2L, indicates that the stages of lithium atoms in these phases are not completely filled.

Fig. 3 shows the measured entropy as a function of lithium composition at 298 K for Li_xC_6. No compensation was made for the small capacity (1.5% of the total cell capacity) of the carbon black filler in the Telcordia cells. The data agree well with the phase diagram of Zheng and Dahn [14,15]. The entropy is constant at −0.1 mV/K for $0.5 < x < 1.0$, corresponding to the transition between stages 1 and 2. The entropy is constant at −0.17 mV/K for $0.25 < x < 0.5$, corresponding to the transition between stages 2L and 2. For lithium stoichiometry below 0.25, there are no further plateaus to indicate a first-order phase transition. Instead, the data show a sloping profile that changes from positive to negative, which may indicate an order–disorder transition similar to what was observed in the lithium–manganese-oxide spinels. This is in agreement with Dahn's report [15] that a two-phase transition is not observed between stages 3L and 4L.

Acknowledgements

This work was supported by the Assistant Secretary for Energy Efficiency and Renewable Energy, Office of Transportation Technologies, Electric and Hybrid Propulsion Division of the US Department of Energy under Contract #DE-AC0376SF00098.

References

[1] D. Bernardi, E. Pawlikowski, J. Newman, J. Electrochem. Soc. 132 (1985) 5.
[2] L. Rao, J. Newman, J. Electrochem. Soc. 144 (1997) 2697.
[3] K.E. Thomas, C. Bogatu, J. Newman, J. Electrochem. Soc. 148 (2001) A570.
[4] R. Darling, J. Newman, J. Electrochem. Soc. 145 (1998) 990.
[5] H.F. Gibbard, J. Electrochem. Soc. 125 (1978) 353.
[6] S. Gross, Energy Convers. 9 (1969) 55.
[7] K.E. Thomas, Lithium-Ion Batteries: Thermal and Interfacial Phenomena, Ph.D. Thesis, University of California, Berkeley, CA, 2002.
[8] K.E. Thomas, S.E. Sloop, J.B. Kerr, J. Newman, J. Power Sources 89 (2000) 132.
[9] O.I. Danilova, I.A. Esikova, S.S. Yufit, Zh. Fiz. Chim. 64 (1990) 129.
[10] J.N. Reimers, J.R. Dahn, J. Electrochem. Soc. 139 (1992) 2091.
[11] M. Menétrier, I. Saadoune, S. Levasseur, C. Delmas, J. Mater. Chem. 9 (1999) 1135.
[12] A. van der Ven, M.K. Aydinol, G. Ceder, Phys. Rev. B 58 (1998) 2975.
[13] I. Saadoune, C. Delmas, J. Solid State Chem. 136 (1998) 8.
[14] T. Zheng, J.R. Dahn, Phys. Rev. B 53 (1996) 3061.
[15] R.J. Dahn, Phys. Rev. B 44 (1991) 9170.